FPGA DESIGN APPROACH OF DIGITAL CONTROL OF THREE-PHASE INDUCTION MOTOR

Cesar da Costa[1], Christian O. Santin[2]
[1]IFSP Federal Institute of São Paulo, São Paulo –SP, Brasil
[2]IFSP Federal Institute of São Paulo, São Paulo – SP, Brasil
E-mail: ccosta@ifsp.edu.br, christianoliveirasantin@hotmail.com

***Abstract*—This paper presents a simulation of a direct torque control (DTC) strategy, which is used to control induction motors. A specific methodology, using MATLAB/Simulink and DSP Builder simulations are presented. It summarizes the prior work before implementation the experimental FPGA control of an induction motor. This methodology allows one to verify the behavior of VHDL codes before their implementations, reducing the risks of significant changes when implemented. The results of the simulations are presented and analyzed in the work.**

Keywords—digital control; induction motor; digital signal processing.

I. INTRODUCTION

The direct torque control (DTC) techniques of three-phase induction motors has gained popularity in industrial applications mainly due to its simple control structure [1, 2]. Several modifications and improvements have been made to the original control structure in order to overcome two major problems normally associated with DTC, namely the high electromagnetic torque ripple and variable switching frequency [1]. It is well established that these problems are mainly due to the use of hysteresis torque and flow controllers. For this reason, most of the methods used to overcome these problems were accomplished by replacing the hysteresis- with the non-hysteresis-based controllers [2, 3, 4].

The study of torque control strategies in three-phase induction motors has attracted a great deal of interest in researchers. Ibrahim et al [5] presented a new proposal to drive DTC using a fuzzy controller, and its results were simulated showing the potential of this strategy. Sandre-Hernandez et al [6] present the implementation of the DTC for a permanent magnet synchronous machine based on the technology of a field programmable gate array (FPGA). Pereira et al [7] propose a virtual teaching platform of DTC of induction motors to assist in the education of undergraduate students. Today, the rapid development in high-performance digital signal processors (DSP) not only replaced the analog technology of the conventional control method but also provides high computing capabilities. Recent developments in FPGA [6, 8] have made it possible to combine complex analog and digital circuits. However, in motion control systems, FPGA technology is not that popular.

The contribution of this work is the development of a digital controller with a DTC algorithm applied to a three-phase induction motor using VHDL embedded in an FPGA, thanks to its parallel architecture for multiple-signal processing.

This paper is organized as follows. Section 2 gives a brief description of three-phase induction motor, and the mathematical model of the induction motor. Section 3 presents a brief description of voltage source inverter. Section 4 presents the principle of direct torque control. Section 5 presents software simulation platform and the DTC strategy simulation. Section 6 presents the test results simulation. Finally, section 7 presents the conclusion.

II. THREE-PHASE INDUCTION MOTOR

The behavior of three-phase induction motors is usually 5escribed by their voltage and current equations. The coefficients of the differential equations that describe their behavior are time varying (except when the rotor is stationary). The mathematical modeling of such a system tends to be complex since the flow linkages, induced voltages, and currents change continuously as the electric circuit is in relative motion. For the analysis of such a complex electrical machine, mathematical transformations are often used to decouple variables and to solve equations involving time varying quantities by referring all variables to a common frame of reference [1, 6]. Among the various transformation methods available, the well-known ones are the Clarke transformation and Park transformation.

The Clarke transformation converts balanced three-phase quantities (a,b,c) into balanced two-phase quadrature quantities (α,β). The Park transformation converts vectors in a balanced two-phase orthogonal stationary system into an orthogonal rotating reference frame (d, q). Clarke and Park transformations are mainly used in vector control architectures related to permanent magnet synchronous machines and asynchronous machines [6]. The three-phase quantities are translated from the three-phase reference frame to the two-axis orthogonal stationary reference frame using the Clarke transformation as shown in Figure 1. Equations 1 and 2 express the Clarke transformation.

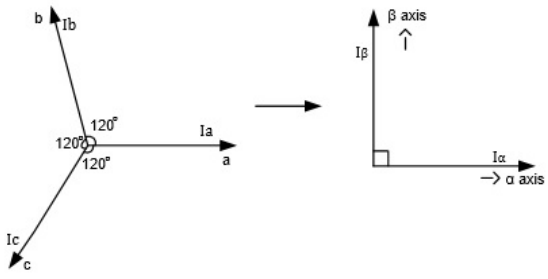

Fig. 1. Clark transformation from three phases to two phases.

$$I_\alpha = \frac{2}{3}(I_a) - \frac{1}{3}(I_b - I_c) \quad (1)$$

$$I_\beta = \frac{2}{\sqrt{3}}(I_b - I_c) \quad (2)$$

Where I_a, I_b and I_c are the three-phase quantities, and I_α and I_β are the stationary orthogonal reference frame quantities.

When I_α is superposed with I_a, and when $I_a + I_b + I_c = 0$, the three-phase quantities I_a, I_b, and I_c can be transformed to I_α and I_β such that $I_\alpha = I_a$, and:

$$I_\beta = \frac{1}{\sqrt{3}}(I_a + 2I_b) \quad (3)$$

The transformation from a two-axis orthogonal stationary reference frame to a three-phase stationary reference frame is accomplished using an Inverse Clarke transformation [6]. The matrix to transform the three vectors V_a, V_b and V_c into V_α, V_β is:

$$\begin{bmatrix} V_\alpha \\ V_\beta \end{bmatrix} = \frac{2}{3}\begin{bmatrix} 1 & \frac{-1}{2} & \frac{-1}{2} \\ 0 & \frac{\sqrt{3}}{2} & \frac{-\sqrt{3}}{2} \end{bmatrix}\begin{bmatrix} V_a \\ V_b \\ V_c \end{bmatrix} \quad (4)$$

A. Mathematical Model of the Induction Motor

The magnitudes involved in the fundamental expressions of motor voltage are related both to the reference of the stator and to the reference of the rotor. Thus, it is necessary to obtain a single and common reference for the stator and rotor. As the DTC technique controls stator quantities, such as currents, voltages, and flow, to facilitate the mathematical modeling of MIT, we adopted the stationary reference. All the values evaluated are based on the mathematical model of the motor in a steady-state condition.

Equation 5 presents the space vector of the stator voltage ($\vec{v}_{s\alpha\beta}$) where $\vec{i}_{s\alpha\beta}$ is the space vector of the stator current, $\vec{\psi}_{s\alpha\beta}$ is the concatenated stator space flow vector, R_s is the winding resistance of a stator phase.

$$\vec{v}_{s\alpha\beta} = R_s \vec{i}_{s\alpha\beta} + \frac{d}{dt}\vec{\psi}_{s\alpha\beta} \quad (5)$$

Equation 6 shows the space vector of the rotor voltage ($\vec{v}_{s\alpha\beta}$) where R_r is the resistance of one rotor phase (equivalent winding) to the stator, $\vec{i}_{r\alpha\beta}$ is the space vector of the rotor current, $\vec{\psi}_{r\alpha\beta}$ is the concatenated rotor flow space vector, Z_p is the pole pair number, w_{mec} is the mechanical speed of the motor.

$$\vec{v}_{r\alpha\beta} = R_r \vec{i}_{r\alpha\beta} + \frac{d}{dt}\vec{\psi}_{r\alpha} - j(Z_p \omega_{mec})\vec{\psi}_{r\alpha\beta} \quad (6)$$

Equation 7 ($\vec{\psi}_{s\alpha\beta}$) is the concatenated stator space flow vector where L_S is the stator inductance, L_H is the mutual inductance between stator and rotor, $\vec{i}_{s\alpha\beta}$ is the space vector of the stator current, and $\vec{i}_{r\alpha\beta}$ is the space vector of the rotor current.

$$\vec{\psi}_{s\alpha\beta} = L_s \vec{i}_{s\alpha\beta} + L_H \vec{i}_{r\alpha\beta} \quad (7)$$

Equation 8 presents the concatenated rotor flow space ($\vec{\psi}_{r\alpha\beta}$) where L_H is the mutual inductance between stator and rotor, L_R is the rotor inductance, $\vec{i}_{s\alpha\beta}$ is the space vector of the stator current, and $\vec{i}_{r\alpha\beta}$ is the space vector of the rotor current.

$$\vec{\psi}_{r\alpha\beta} = L_H \vec{i}_{s\alpha\beta} + L_r \vec{i}_{r\alpha\beta} \quad (8)$$

In the Equation 9 (m_d) is the electromagnetic torque where Z_p is the pole pair number, $\psi_{s\alpha}$ is the component α of stator flow, $i_{s\beta}$ is the component β of stator current, $\psi_{s\beta}$ is the component β of Stator flow, and $i_{s\alpha}$ is the component α of stator current.

$$m_d = \frac{3}{2} Z_p (\psi_{s\alpha} i_{s\beta} - \psi_{s\beta} i_{s\alpha}) \quad (9)$$

III. VOLTAGE SOURCE INVERTER

The topology of a voltage source inverter (VSI) is comprised of six insulated gate bipolar transistors (IGBTs) and six freewheeling diodes [5, 6, 7]. According [6], the topology of a voltage source inverter (VSI) is a shown in Fig. 2.

Assuming that in every instant the switching devices can accept only one of the two possible states on (1) or off (0), the VSI has only eight possible switching states, generating six active voltage space vectors (AVSVs) v_1 a v_6 and two zero voltage space vectors (ZVSVs) v_0 e v_7. Using the Clarke transformation given by Equation 4, the states of the inverter can be mapped onto the α-β complex plane, which are shown in Fig. 3.

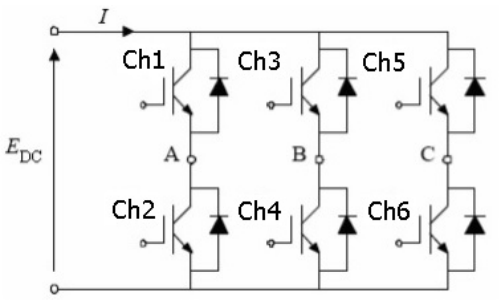

Fig. 2. Scheme of Voltage Source Inverter (VSI).

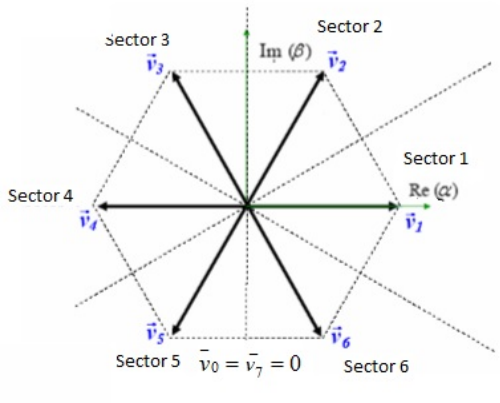

Fig. 3. Voltage space vectors generated by the VSI.

The space sector N is obtained from the angle $\delta_{\psi s}$ between the stationary reference and the stator flow (Equation 10), and is limited by Equation 11:

$$\delta_{\psi s} = tg^{-1}\left(\frac{\psi_{s\beta}}{\psi_{s\alpha}}\right) \tag{10}$$

$$(2N-3)\frac{\pi}{6} < \delta(\mathrm{N}) < (2N-1)\frac{\pi}{6} \tag{11}$$

Where N is the space sector, and δ is the space angle.

IV. Principle of Direct Torque Control

A summary block diagram of the DTC technique is presented in Fig. 4 using hysteresis comparators, a motor estimation model, and switching logic. The main objective of this technique is to control the torque and the flow of the stator using the comparators, ensuring a fast torque response. The vector table is used to select the voltage vector to be applied to the stator, determined the switches that must be activated in the inverter (space modulation). The choice of the voltage vector is made to maintain the stator torque and flow within the limits defined by the hysteresis comparators. There are six possible AVSVs $(\vec{v_1}\ a\ \vec{v_6})$ and two ZVSVs $(\vec{v_0}\ e\ \vec{v_7})$, which are chosen based on the error between the torque (Γ) and flow (Φ) reference values and the spatial sector of the stator flow ($tg^{-1}\left(\frac{\psi_{s\beta}}{\psi_{s\alpha}}\right)$).

The currents measured at the motor input (i_a, i_b) are inputs from the "motor model" block, which estimates the torque and the stator flow at that instant, in addition to the space sector where the stator flow is located. The estimated stator torque (m_d) and flow ($\psi_{s\alpha\beta}$) are compared to their respective references (m_{dref}, ψ_{sref}). Comparison errors are inputs from the hysteresis comparators (usually two levels for the flow and three levels for the torque), which verify that the torque and flow are within their given limits. The outputs of these comparators (Γ and Φ), as well as the stator flow space sector, are inputs from the "Vector Table," which determines the proper switching of the inverter to maintain stator flow and torque close to its reference values

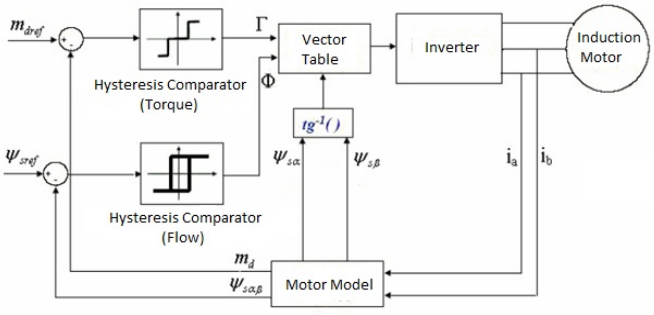

Fig. 4. Structure of direct torque control system

The Table 1 presents the table of voltage vectors to be applied to the inverter [1, 6, 7].

V. Simulate Plataform Software

The simulation platform consists of two software programs: MATLAB/Simulink and DSP Builder. MATLAB/Simulink is responsible for simulating the power part of the drive and control, whereas the DSP Builder software converts the MATLAB/Simulink codes to the VHDL language and allows the loading of the codes into the FPGA device [8].

The architecture of the DTC scheme is shown in Fig. 4. The control system includes a Clark transformation, motor model algorithm, flux and torque estimation, sector determination, hysteresis-band controllers for torque and flux, the optimum

switching vector table. All modules have been described using VHDL language.

TABLE I
Switching Table Voltage Vectors

Φ	Γ	Sec1	Sec2	Sec3	Sec4	Sec5	Sec6
0	1	v_2	v_3	v_4	v_5	v_6	v_1
	0	v_7	v_0	v_7	v_0	v_7	v_0
	-1	v_6	v_1	v_2	v_3	v_4	v_5
1	1	v_3	v_4	v_5	v_6	v_1	v_2
	0	v_0	v_7	v_0	v_7	v_0	v_7
	-1	v_5	v_6	v_1	v_7	v_3	v_4

The full architecture has been tested using the software DSP Builder simulations on an Altera DE2-115 board with a Cyclone IV EP4CE115 device, in this way, the control is loaded into the FPGA to run in real time while the machine is simulated using the MATLAB/Simulink. Fig. 5 illustrates the design flow with the MATLAB/Simulink and DSP Builder software.

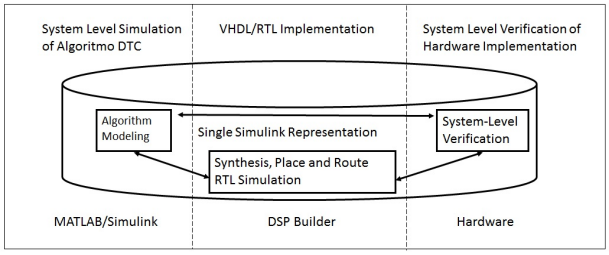

Fig.5. Design flow with the MATLAB/Simulink and DSP Builder.

Fig. 6 illustrates the conversion process of the DSP application graphic model, created in SIMULINK® with DSP Builder® libraries, into VHDL hardware description code.

A. DTC Strategy Simulation

According to the DTC structure shown in Figure 4, the motor model block, estimation of flow and torque block, current acquisition, and inverter block are performed and simulated in the MATLAB/Simulink environment. Stator torque and flow controls are performed using the torque hysteresis comparator and flow hysteresis comparator block, which are, along with the vector table block, implemented and simulated in the DSP Builder software.

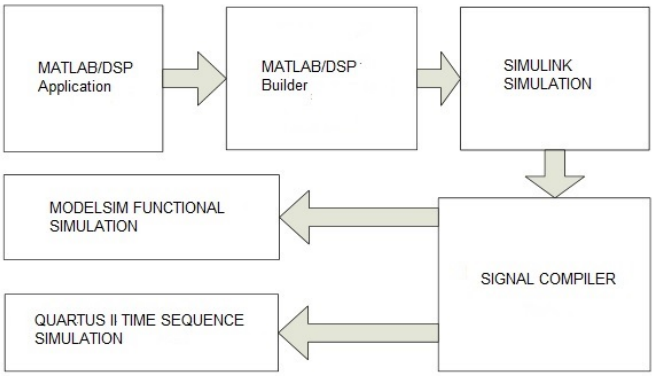

Fig. 6. Conversion process of the graphic model - Simulink of a DSP application in VHDL code

In the DTC control algorithm block, the motor model calculations and their respective comparisons with their reference values are performed, in addition to determining the space sector where the flow is. The outputs of the hysteresis comparators, in addition to the spatial flow sector, are inputs to the part of the program responsible for the inverter-switching table. This table indicates the best alternative for the DTC at that instant and triggers the inverter keys to maintain the desired control.

The simulated inverter uses switches, since the IGBT transistors are considered as switches for the frequency level used in the simulation. The switching frequency chosen was 20 kHz. The instrumentation part (A/D converter) was performed and simulated in the MATLAB/Simulink environment. Stator currents enter as binary data in the DTC control algorithm. For resolution of the A/D converter, 16 bits were assumed. The sampling frequency used in the A/D converter was 40 kHz. The control algorithm that controls the motor based on the DTC strategy has been divided into two parts. The first part, responsible for calculations, operates at a frequency of 40 kHz. The second part, which contains the inverter-switching table, operates at a frequency of 20 kHz

Parameters of induction motors used in the simulation are listed in Table 2. Figure 7 shows the DTC strategy simulation.

TABLE II
Parameter of Induction Motor

Parameter	*Value*	*Parameter*	*Value*
Rated torque	10 Nm	Pole pairs	2
Stator resistance	7,56 Ω	Rotor resistance	3,84 Ω
Stator inductance	0,35 H	Rotor inductance	0,35 H
Rated power	1,5 Hp	Flux linkage	0,8 Wb
Rotor inertia	0,027 Kgm^2	Load torque	6 N
Mutual inductance	0,33 H	Coefficient of friction	0,00012

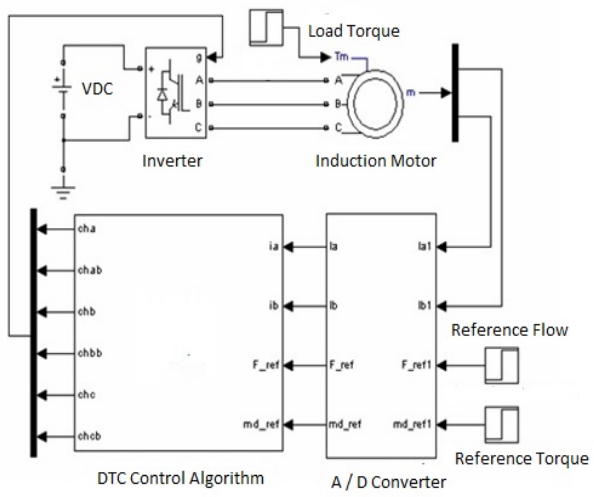

Fig.7. DTC strategy simulation.

VI. TEST RESULTS SIMULATION

In order to verify the proposed DTC strategy, simulation results are presented. The Altera DE 2 board with a Cyclone III device is used to execute the DTC control algorithm. Fig. 8 shows the simulation result of the DTC algorithm for positive and negative references of the magnitude of the estimated stator flow and its reference. Fig. 9 shows the simulation result of the DTC algorithm for positive and negative references of the estimated electromagnetic torque and its reference. To perform the test of DTC, a positive reference torque is applied to the induction motor with a reference of zero N·m during the initial time, and 10 N·m at 0.25 s.

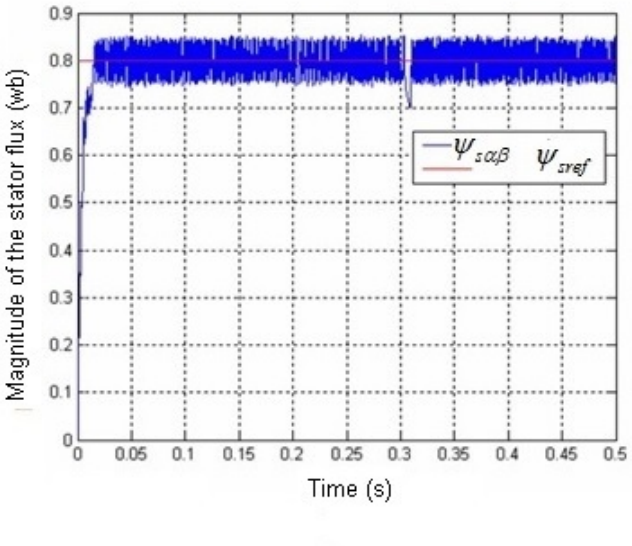

Fig. 8. Simulation results of stator flow estimated.

Fig. 10 shows the simulation result of the DTC algorithm for positive and negative reference of stator currents. In Figure 10 (a), a change can be observed between two phases at a time equal to 0.25 s due to the change in the torque direction of the motor. The period between the instants 0.3 s and 0.4 s shows the behavior of the phase currents when the velocity is reduced. In Figure 10 (b), the rate of growth of the motor speed is changed at 0.1 s when a load of 6 N·m is coupled to the shaft. At a time of 0.25 s, the torque reference changes direction, causing the motor speed to decrease and after a short time interval it change its direction of rotation.

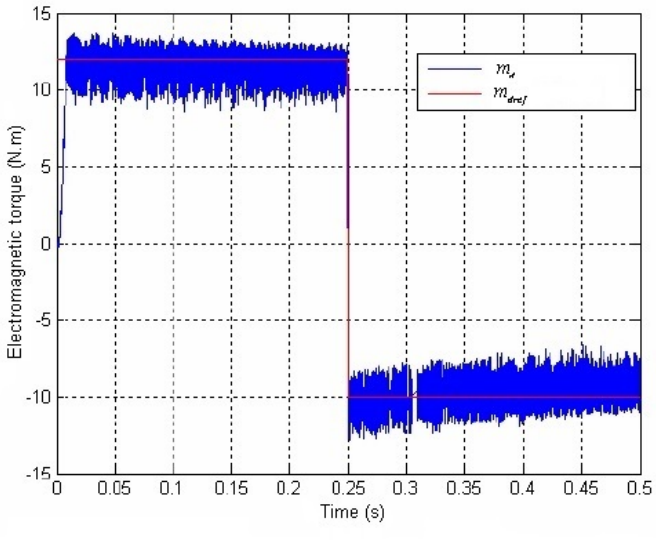

Fig. 9. Simulation results torque estimated.

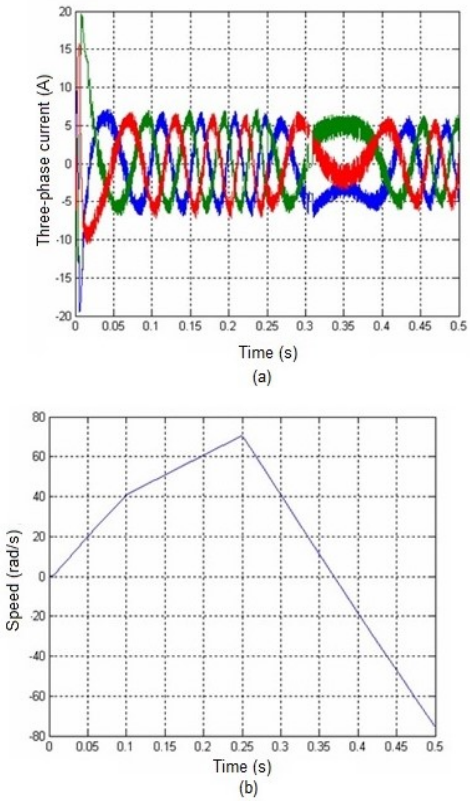

Fig. 10. (a) Simulation results of three-phase stator currents, and (b) Motor Speed by the proposed DTC algorithm

VII. CONCLUSION

This paper has presented the digital design and simulation of the DTC strategy using VHDL language. A DSP design for motor control has been developed and simulated for the particular case of the DTC algorithm of a three-phase induction motor. A specific methodology, using software configurations and a mixed simulation, allowed the verification of the behavior of the VHDL codes before their implementations on the FPGA device. The methodology defined the digital adaptation of the DTC algorithm, taking account of the influences of digitization on computed values. An optimized DSP algorithm and a specific fixed-point format have been studied and defined. The implementation, which proved that the DTC strategy, was accomplished using the combination of a MATLAB/Simulink and DSP Builder software. This project addressed a way of structuring and simulating a DTC algorithm. The target technology was FPGAs, which have been growing steadily and has been taking up space in the industrial market worldwide.

REFERENCES

[1] D. Casadei, G. Serra, A. Tani, L. Zarri, "Direct torque control for induction machines: a technology status review", 2013 IEEE Workshop on Conference Electrical Machines Design Control and Diagnosis (WEMDCD), 2003, pp. 117–129.

[2] F. Niu; B. Wang; A. S. Babel; K. Li, E.G. Strangas, "Comparative Evaluation of Direct Torque Control Strategies for Permanent Magnet Synchronous Machines," in Power Electronics, IEEE Transactions on, vol.31, no.2, 2016, pp.1408-1424.

[3] P. Matic, S. N. Vukosavic, "Direct Torque Control of Induction Motor in Field Weakening Without Outer Flux Trajectory Reference", International Review of Electrical Engineering, Vol. 6, No.3, 2011, pp: 1204-1212.

[4] S. N. Pandya, J. K. Chatterjee, "Torque ripple reduction in direct torque control based induction motor drive using novel optimal controller design technique", Power Electronics, Drives and Energy Systems (PEDES) & 2010 Power India, 2010 Joint International Conference on , pp:20-23. Doi**:** 10.1109/PEDES.2010.5712449.

[5] S. O. Ibrahim, K. N. Faris, E. A. Elzahab, "Implementation of fuzzy modeling system for faults detection and diagnosis in three phase induction motor drive system". Journal of Electrical System and Information Technology 2 (2015)27-46.

[6] O. Sandre-Hernandez, J. J. Rangel-Magdaleno, R. Morales-Caporal, "Implementation of direct torque control for a PM synchronous machine based on FPGA". 13th International Conference on Power Electronics (CIEP), 2016, pp. 155-160.

[7] W. C. A. Pereira, M. L. Aguiar, G. T. Paula, , J. R. B. A. Monteiro, G. H. Bazan, M. F. Castoldi, D. S. Sanches, " Virtual Platform of direct torque control of induction motor to assist in education of undergraduate students". 2015 IEEE 24th International Symposium on Industrial Electronics (ISIE), 2015, pp. 814-818.

[8] C. Da Costa, M. Kashiwagi, M. H. Mathias, "Digital systems design based on DSP algorithms in FPGA for fault identification in Rotary machines". Journal of Mechanics & Industry, v.2, 2014, pp. 1-5.